Proceedings World Geothermal Congress 2000
Kyushu - Tohoku, Japan, May 28 - June 10, 2000

THREE - DIMENSIONAL MAGNETOTELLURIC INVESTIGATION IN KAKKONDA GEOTHERMAL AREA, JAPAN

Kazunobu Yamane[1], Kazumi Ohsato[1], Takao Ohminato[2] and Hee Joon Kim[3]
[1]Geothermal Energy Research and Development Co., Ltd. , Tokyo 103-0026, Japan.
[2]New Energy and Industrial Technology Development Organization., Tokyo 170-6028, Japan.
(Now: Earthquake Research Institute, University of Tokyo, 1-1-1, Yayoi, Bunkyo-ku, Tokyo, Japan)
[3]Pkyung National University, Pusan 608-737, Korea.

Key Words: magnetotelluric, geothermal, three dimension, inversion

ABSTRACT

The New Energy and Industrial Technology Development Organization (NEDO) began the Deep Geothermal Resources Survey (DSGR) program in 1992. The objective is to attain fundamental knowledge about deep geothermal systems at the Kakkonda geothermal field, Japan. As part of the DSGR project, three-dimensional magnetotelluric (MT) inversion was studied for actual exploration activities. Thus, we have developed a generalized rapid relaxation inversion (GRRI) method to interpret MT data. The GRRI method is extremely fast because it allows separate one-dimensional (1-D) inversions for updating the conductivity structure. We have derived this scheme based on a locally 3-D analysis to improve the computational efficiency and stability of inversion. The developed algorithm has been realized in the GRRI-3D code, which has been tested by synthetic 3-D MT data. It clearly demonstrates the utility of the high-dimensional MT inversion, and enhances a complex and realistic 3-D conductivity mapping capability.

In 1998, a 3-D MT survey was conducted in Kakkonda geothermal field located in Iwate prefecture, Japan. GRRI-3D algorithm was applied to these MT data and a resistivity structure of Kakkonda geothermal field recovered.

1. INTRODUCTION

Three-dimensional magnetotelluric (MT) inversion may be one of the formidable tasks in electromagnetic exploration. Recently, 3-D MT inversion has been studied to delineate 3-D geological structures. Most of these studies, however, require enormous computational resources. One of the promising approaches may be the rapid relaxation inversion RRI (Smith and Booker, 1991) method where the actual inversion is carried out for each column in 1-D fashion. The forward modeling used may be rigorous, so that as iteration is continued one hopes to have the lateral effects gradually accounted for.

Lee *et al* (1995) and Yamane *et al* (1998) developed recently an approach to the 2-D inversion of MT data, and named their method GRRI (Generalized RRI). Although the GRRI scheme does not require additional computation time when compared with the RRI scheme, it should converge faster with less likely getting caught in local minima. This is because this method involves a local 2-D analysis, but the inversion part of the original RRI is strictly 1-D. We have extended the GRRI scheme to solve 3-D MT problems.

In this paper it is expected that the data structure be completely in the form of tensor impedance and admittance, and that the base of data encompasses over a 2-D surface area. In the initial development of 3-D MT inversion scheme, we used the finite-difference forward code developed by Mackie *et al* (1994). However, the inversion code named GRRI3D should be able to utilize any 3-D forward code as long as it is efficient in terms of computing speed with reasonably accurate modeling results.

Kakkonda MT data acquired in 1998 is used for 3-D inversion analysis. MT soundings have been made at 76 locations in and around the Kakkonda geothermal field. Within the field a conductive layer at variable depth is underlain by a more resistive layer.

2. KAKKONDA MT SURVEY

The Kakkonda geothermal field is situated on the western edge of Iwate prefecture of Japan. From July through September in 1998 we collected MT data at 76 sites in Kakkonda area (Figure 1). The survey was planned in the form of four profiles in order to account for the 3-D effects. There are, however, several power lines, geothermal facilities and a power plant along the Kakkonda river, so we skipped such areas to avoid contaminating MT data with noise. Each profile was aligned N70E, because the folding of Miocene formations occurred in NNW-SSE to NW-SE directions.

The Kakkonda MT data is measured over a frequency range 125-0.001Hz with remote reference. The electric dipoles are orientated parallel to and normal to the traverse with 200m length. The magnetic field is acquired over the same frequency range with two horizontal induction coils oriented parallel to and normal to the traverse direction. The data were processed using cascade decimation algorithm, which is suitable for fast calculations over a wide frequency band like Kakkonda MT dataset. After the time series data were processed using the cascade decimation method and the Fourier coefficients were obtained, power spectra were calculated. The data were sorted by the multiple coherency between appropriate horizontal field components in this time. In our processing scheme, a coherency-sorting algorithm was added to the original cascade decimation. First, incoming data are passed through operator-specified minimum amplitude screening criteria, based on the magnetic field amplitude of 6^{th} and 8^{th} Fourier coefficients from the cascade decimation. The auto power spectra and cross power spectra are calculated from the Fourier coefficients and sorted in temporary storage at each level of decimation. When the number specified for averaging is reached at a given level of decimation, four multiple coherencies are calculated for each harmonic. The average of the spectra is then sorted and accumulated into a file based on the value of the geometric mean of the H-E_X and E-H_Y coherencies and of the H-E_Y and E-H_X coherencies. The storage file into which the temporary spectral averages are sorted is divided into ten bins, each containing complete data sets from which MT parameters can be calculated, with different data quality based on the multiple coherencies.

Showing only representative sites helped to simplify the interpretation and understanding of major trends in the data. For example, data from sites #7 in line-C and #5 in line-D are similar (Figure 2). Both sites are located along the Kakkonda river, and show the divergence of the apparent resistivity curves of XY and YX mode below 1.0Hz, suggesting a higher dimensional structure at depth.

3. THEORETICAL DESCRIPTION OF INVERSION

From Maxwell's equation in the frequency domain, one derives the following Helmholtz equation in terms of the electric field.

$$\nabla \times \nabla \times \mathbf{E} + i\omega\mu\sigma\mathbf{E} = 0 \tag{1}$$

Taking the perturbation of this equation with respect to the conductivity, we obtain

$$\nabla \times \nabla \times d\mathbf{E} + i\omega\mu\sigma\, d\mathbf{E} = -i\omega\mu\, d\sigma\, \mathbf{E} \tag{2}$$

Suppose that the 3-D model is divided into a set of vertical prisms (Figure 3). We choose nine neighboring prisms as the basic inversion unit. This unit consists of the volume V whose surface boundary is composed of top boundary (TBV) and four side boundaries (SBV). The bottom boundary may be ignored since we will assume that electric and magnetic field are negligibly small.

Now we define a test function, E*, such that

$$\mathbf{E}^* = \begin{cases} \mathbf{E} & \text{in } V_1, \\ \mathbf{0} & \text{on } SBV, \end{cases} \tag{3}$$

Multiplying the perturbed field equation (2) by the test function E* and integrating over the volume, we get

$$\int_V (\nabla \times \nabla \times d\mathbf{E} + i\omega\mu\sigma d\mathbf{E}) \cdot \mathbf{E}^* dv = -\int_V i\omega\mu d\sigma \mathbf{E} \cdot \mathbf{E}^* dv \tag{4}$$

Integrating by parts of the equation, or applying the Green theorem, this equation is broken into

$$\oint_{BV} [(\mathbf{n}\times\nabla\times d\mathbf{E}) \cdot \mathbf{E}^* - (\mathbf{n}\times\nabla\times\mathbf{E}^*) \cdot d\mathbf{E}] da + \int_V (\nabla\times\nabla\times\mathbf{E}^* + i\omega\mu\sigma\mathbf{E}^*) \cdot d\mathbf{E} dv = -\int_V i\omega\mu d\sigma \mathbf{E} \cdot \mathbf{E}^* dv \tag{5}$$

where **n** is a unit vector outward normal to BV (Figure 3). According to the definition of test function **E*** described by equation (3), equation (5) is finally reduced to

$$\begin{aligned} \int_{V_1} d\sigma (E_x^2 + E_y^2 + E_z^2) dv = & \int_{TBV} [(dH_y E_x^* - dH_x E_y^*) + (dE_y H_x^{**} - dE_x H_y^{**})] da \\ & + \frac{1}{i\omega\mu} \oint_{SBV} (\mathbf{n} \times \nabla \times \mathbf{E}^*) \cdot d\mathbf{E}\, da \\ & - \int_{V_2} \left(\sigma \mathbf{E}^* + \frac{\nabla \times \nabla \times \mathbf{E}^*}{i\omega\mu} \right) \cdot d\mathbf{E}\, dv \\ & - \int_{V_2} d\sigma\, (E_x E_x^* + E_y E_y^* + E_z E_z^*) dv \end{aligned} \tag{6}$$

We limit the only unknown to be the conductivity variation in the central prism V_1 on right-hand side of the above equation. If the prism V_1 consists of K blocks, a discretized version of equation (6) is

$$\sum_{k=1}^{K} C_v(x_i, y_j, z_k; w)\, d\sigma_m(x_i, y_j, z_k) = S \tag{7}$$

Here, $\delta\sigma_m$ is the incremental change in the log conductivity for each element in V_1. C is the kernel of the integral equation.

4. SYNTHETIC TEST

In order to test the effectiveness of this inversion scheme, we selected a simple model, shown in Figure 4. Two conductive prisms are surrounded by homogeneous earth with 100 ohm-m. The frequencies used for this model are 1000, 500, 200, 100, 50, 20 and 10Hz. The inverse model used here comprises 324 (=18 x 18) columns of 20 x 20 x 315 m, and each column has ten layers. The inversion procedure is repeated until a misfit between the measured and modeled data is reduced to an acceptable level of rms misfit (*S*), which is given by

$$S = \sqrt{\frac{1}{N} \sum_{i=1}^{N} \frac{\left\| \mathbf{Z}_i^m - \mathbf{Z}_i^d \right\|^2}{\left\| \mathbf{Z}_i^d \right\|^2}} \tag{8}$$

where $\|\bullet\|$ denotes the determinant, **Z** is the impedance tensor, and the superscripts *m* and *d* indicate the modeled and measured data, respectively. If we choose an appropriate damping factor, then a reasonable inversion result can be obtained after several iterations. Figure 5 shows an example of successful inversion, and the inverted image was obtained after ten iterations. The residual error was reduced from 0.01 to 0.001 and changed insignificantly after ten iterations as shown in Figure 4. From Figure 5 we can find that the two conductors are clearly identified. In the inversion all the resistivity parameters are constrained to positive values.

5. 3-D RESULT

The geology of Kakkonda area consists of a Miocene formation, the Tamagawa welded tuff, Quaternary andesite lavas and pyroclastic rocks, and many dyke rocks intruded into the Miocene formation. Recently, a granite pluton has been confirmed ia a well of 2,000-3,000m depth, which is considered to be a possible heat source of Kakkonda area (Doi *et al*, 1998).

We use MT data from a total of 76 MT soundings in the inversion. The frequencies used here range from 0.01 to 120Hz. Data below 0.01Hz is neglected. This is because the depth of interest is about 4km depth in term of the each traverse's length.

A relatively conductive zone (20 ohm-m or less) is extensively found from the surface to about 1.5km. This zone seems to correspond to a hydrothermally altered zone and Miocene sedimentary rocks, which are widely distributed at these levels. On the other hand, a resistive zone may be dominant below this formation. This resistive body may correspond to the granite.

6. CONCLUSIONS

We applied the 3-D MT inversion algorithm on a simple synthetic model and the Kakkonda geothermal field. In the first stage, intensive data processing using cascade decimation was carried out in order to obtain a high quality impedance data set for 3-D analysis. The algorithm of the MT inversion described here is similar to the boundary element method. The test function is forced to take zero value on the four side boundaries of a nine prisms inversion unit to render the resulting perturbation equation easy to handle. This method approximates conductivity mapping. However, it is possible to reconstruct 3-D resistivity images with a small amount of computer resources.

We could delineate the deep subsurface structure of Kakkonda geothermal

field, with shallow resistivity distribution regarded as due to an altered zone and Miocene sedimentary rocks.

REFERENCES

Doi, N., Kato, O., Ikeuchi, K., Komatsu., R.., Miyazaki, S., Akaku, K., and Uchida, T. (1998). Genesis of the plutonic-hydrothermal system around Quaternary granite in the Kakkonda geothermal system, Japan. *Geothermics*, Vol.27, pp.663-690.

Lee, K.H., Xie, G., Yamane, K., and Takasugi, S. (1995). A new 2-D inversion scheme for magnetotelluric data using a modified RRI method. *Proc. World Geothermal Congress,* Florence, Italy, 1995.

Mackie, R.L. and Madden, T.R. (1994). Three-dimensional magnetotelluric inversion using conjugate gradients. *Geophys. J. Int.*, Vol.115. , pp.215-229.

Smith, J.T. and Booker, J. R. (1991). Rapid inversion of two- and three-dimensional magnetotelluric data.. *J. Geophys. Res*., Vol.96, pp.3905-3922.

Takasugi, S., Tanaka, K., Kawakami, N., and Muramatsu, S. (1992). High spatial resolution of resistivity structure revealed by a dense network MT measurement - a case study in the Minamikayabe area, Hokkaido, Japan. *J. Geomag. Geoelectr*., Vol.44, pp.289-308.

Yamane, K., Takasugi, S., Lee, K.H., and Ashida, Y. (1998). A new magnetotelluric inversion scheme using generalized RRI method and case studies. *Butsuri-Tansa*, Vol.51, pp.141-153.

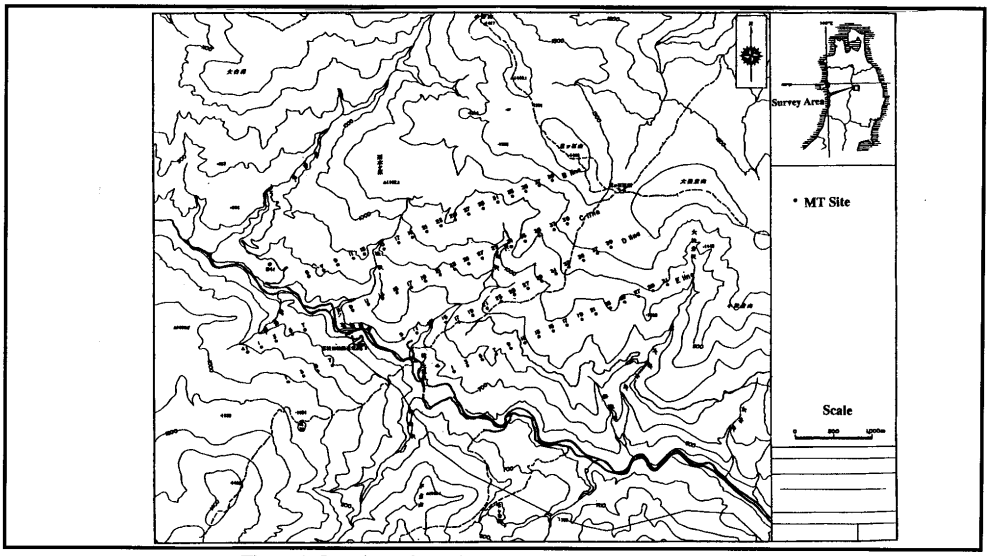

Figure 1. Locations of MT sites across the Kakkonda geothermal field

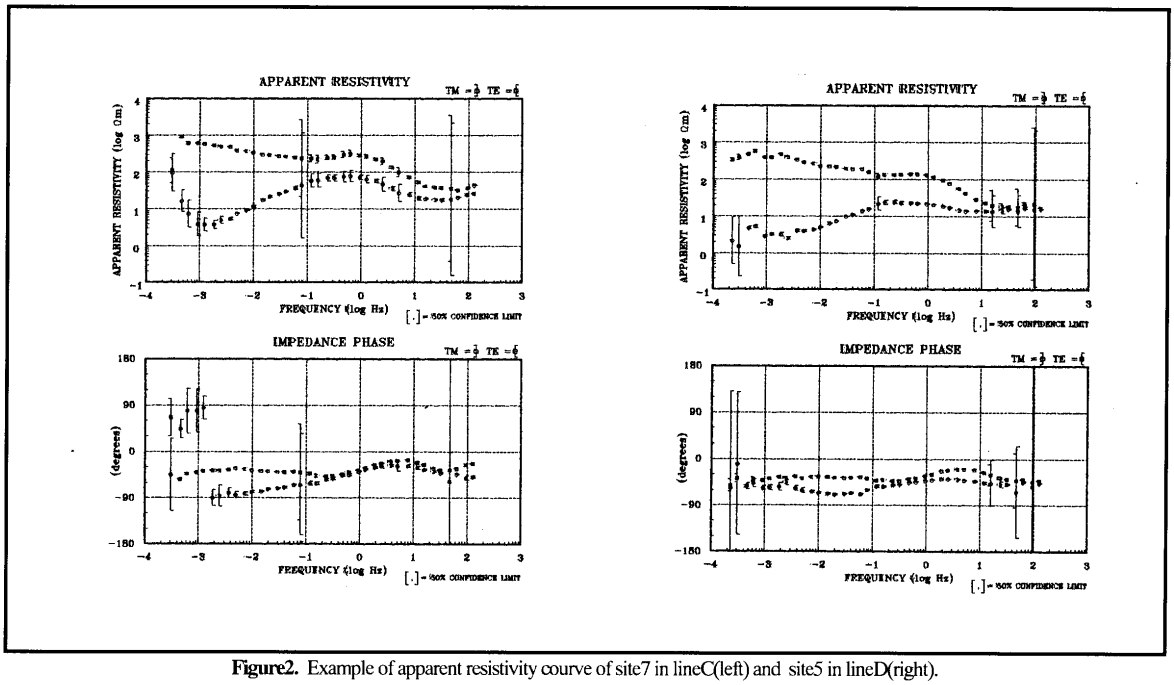

Figure2. Example of apparent resistivity courve of site7 in lineC(left) and site5 in lineD(right).

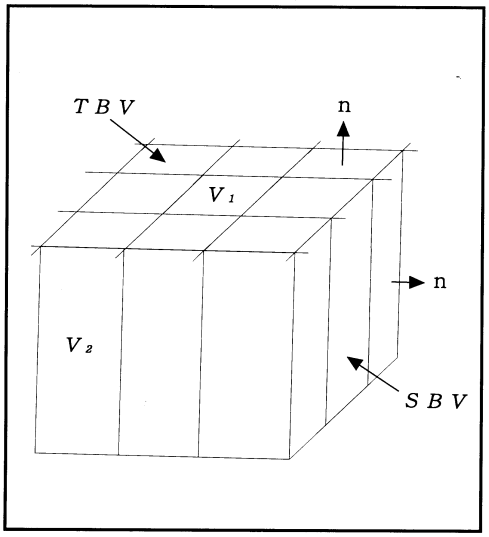

Figure3. Inversion Unit for GRRI3-D

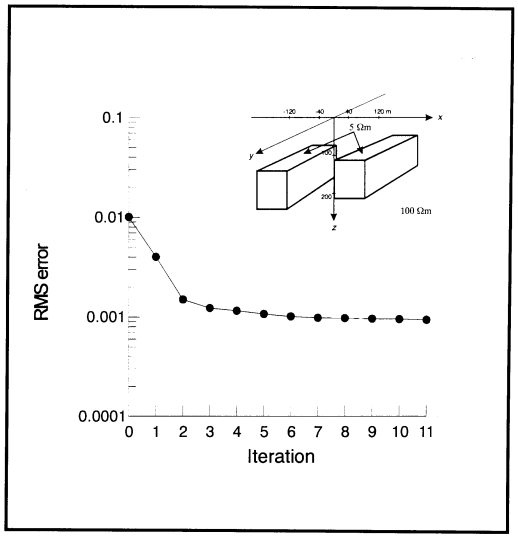

Figure 4. Synthetic model with two conductive bodies and *RMS* error

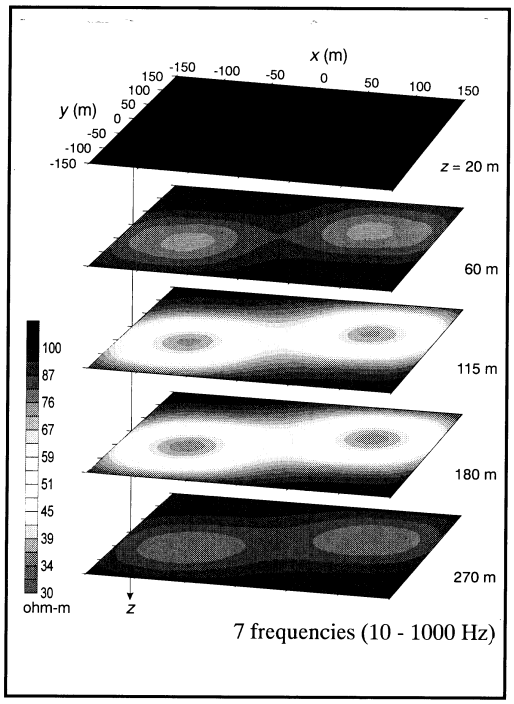

Figure5. Inverted image of the synthtic data

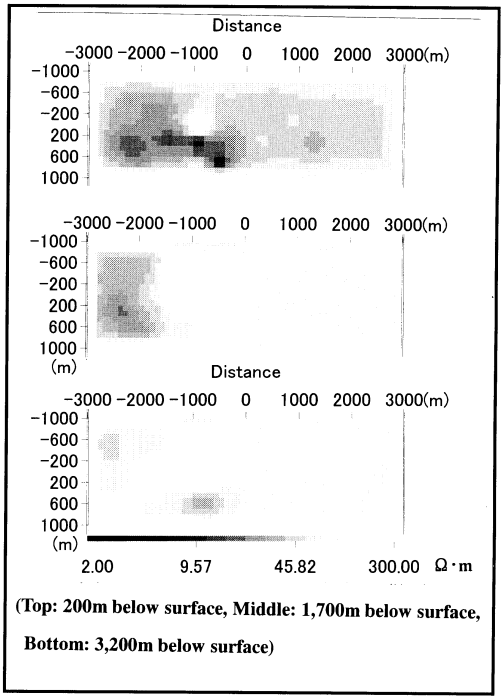

Figure 6. Inversion result of Kakkonda MT data